THE JOURNAL OF BIOLOGICAL CHEMISTRY VOL. 283, NO. 34, pp. 23244–23253, August 22, 2008

Guanine Nucleotide Exchange Factor Independence of the G-protein eEF1A through Novel Mutant Forms and Biochemical Properties*

Received for publication, February 11, 2008, and in revised form, June 17, 2008 Published, JBC Papers in Press, June 18, 2008, DOI 10.1074/jbc.M801095200

Sedide B. Ozturk and Terri Goss Kinzy[1]

From the Department of Molecular Genetics, Microbiology, and Immunology, University of Medicine and Dentistry of New Jersey Robert Wood Johnson Medical School, Piscataway, New Jersey 08854

Most G-proteins require a guanine nucleotide exchange factor (GEF) to regulate a variety of critical cellular processes. Interestingly, a small number of G-proteins switch between the active and inactive forms without a GEF. Translation elongation factor 1A (eEF1A) normally requires the GEF eEF1Bα to accelerate nucleotide dissociation. However, several mutant forms of eEF1A are functional independent of this essential regulator *in vivo*. GEF-independent eEF1A mutations localize close to the G-protein motifs that are crucial for nucleotide binding. Kinetic analysis demonstrated that reduced GDP affinity correlates with wild type growth and high translation activities of GEF-independent mutants. Furthermore, the mutant forms show an 11–22-fold increase in rates of GDP dissociation from eEF1A compared with the wild type protein. All mutant forms have dramatically enhanced stability at elevated temperatures. This, coupled with data demonstrating that eEF1A is also more stable in the presence of nucleotides, suggests that both the GEF and nucleotide have stabilizing effects on eEF1A. The biochemical properties of these eEF1A mutants provide insight into the mechanism behind GEF-independent G-protein function.

GTPases regulate a variety of cellular functions with a conserved mechanism of nucleotide binding and hydrolysis. Signal transduction, control of cell cycle and differentiation during cell division, protein biosynthesis, vesicular trafficking, and translocation of membrane proteins are key cellular processes where GTPases play critical roles. Based on their functional roles, domain structures, or sizes, the superfamily of GTPases can be divided into many families, including small G proteins (Ras GTPase superfamily), heterotrimeric G proteins, and the translation factor family (1). All GTPases share a G-domain with conserved sequence elements, such as switch I and II, the P-loop (phosphate binding loop), and the NK*X*D element (2). Guanine nucleotides form specific interactions with these sites, which are modulated by G-protein accessory factors to create the switch mechanism between the active and inactive forms (1, 3).

GTPase activation factors stimulate GTP hydrolysis, resulting in the inactive GDP-bound form. Guanine nucleotide exchange factors (GEFs)[2] catalyze GDP release by reducing the nucleotide affinity (1). This allows G-proteins to rebind GTP due to a higher cellular concentration of GTP and thus switch to their active form. The GEFs interact with the switch I and II regions while inserting residues close to or into the P-loop and Mg^{2+} binding site. The insertion of the GEF residues perturbs the interaction surface in the phosphate binding region, resulting in the release of phosphate groups, which in turn causes dissociation of the nucleotide. In contrast to the mechanism of exchange and the G-proteins themselves, GEFs show little to no conservation in sequence or structure (3).

The crystal structures of the majority of G-proteins solved in the presence of nucleotides show that the β-phosphate of the nucleotide interacts with the P-loop, and this interaction is considered to be the most important element for the tight binding of nucleotide (1). Another important contributor to binding affinity and specificity is the NK*X*D element, which interacts with the nucleotide base (2). Until recently, the order of events that leads to nucleotide release and the region of the nucleotide released first were unclear. However, a sequence of interactions was proposed at least for some G-proteins. According to the model, upon binding of the GEF to the G-protein, the phosphate groups are released first, and then the base of the entering nucleotide binds to the NK*X*D motif and displaces the GEF (4).

Although most of the GTPases require a GEF, some G-proteins can function efficiently without an exchange factor. Typically, GEFs accelerate the nucleotide release from G-proteins, which is normally a slow process. A G-protein without a GEF probably allows nucleotide release rapid enough for cell survival. G-proteins could maintain rapid nucleotide release rates that lead to GEF independence in several ways. Lower affinity of GDP for the G-protein could allow a G-protein to function without a GEF. In addition, the G-protein may not require the separate level of regulation of activity typically performed by the GEF. The eukaryotic proteins translation elongation factor 2 (eEF2), release factor 3 (eRF3), initiation factor 5B (eIF5B), selenocysteine-specific elongation factor (eEFSec) and the eEF1A-like GTPases Hbs1p and Guf1p apparently function

* This work was supported, in whole or in part, by National Institutes of Health Grant GM 57483. The costs of publication of this article were defrayed in part by the payment of page charges. This article must therefore be hereby marked "*advertisement*" in accordance with 18 U.S.C. Section 1734 solely to indicate this fact.

[1] To whom correspondence should be addressed: Dept. of Molecular Genetics, Microbiology, and Immunology, UMDNJ Robert Wood Johnson Medical School, 675 Hoes Ln., Piscataway, NJ 08854-5635. Tel.: 732-235-5450; Fax: 732-235-5223; E-mail: kinzytg@umdnj.edu.

[2] The abbreviations used are: GEF, guanine nucleotide exchange factor; eEF1, eEF1A, eEF1B, and eEF2, translation elongation factor 1, 1A, 1B, and 2, respectively; eEFSec, selenocysteine-specific elongation factor; eRF3, eukaryotic release factor 3; eIF5B, eukaryotic initiation factor 5B; FRET, fluorescence resonance energy transfer; mant, 2′-(or 3′)-*O*-*N*-methylanthraniloyl.

TABLE 1
***S. cerevisiae* strains**

Strain	Genotype	Reference
MC213	*MATα ura3-52 leu2-3,112 trp1-Δ1 lys2-20 met2-1 his4-713 tef1::LEU2 tef2Δ tef5::TRP1* p*TEF1 URA3*	19
TKY368	*MATα ura3-52 leu2-Δ1 trp1-Δ101 lys2-801 met2-1 his4-713 tef5::TRP1* pTEF5 *LEU2*	13
TKY961	*MATα ura3-52 leu2-3,112 trp1-Δ1 lys2-20 met2-1 his4-713 tef1::LEU2 tef2Δ tef5::TRP1* p*TEF1 URA3* (R164K)	19
TKY963	*MATα ura3-52 leu2-3,112 trp1-Δ1 lys2-20 met2-1 his4-713 tef1::LEU2 tef2Δ tef5::TRP1 pTEF1 URA3* (T22S)	19
TKY964	*MATα ura3-52 leu2-3,112 trp1-Δ1 lys2-20 met2-1 his4-713 tef1::LEU2 tef2Δ tef5::TRP1 pTEF1 URA3* (A112T)	19
TKY965	*MATα ura3-52 leu2-3,112 trp1-Δ1 lys2-20 met2-1 his4-713 tef1::LEU2 tef2Δ tef5::TRP1 pTEF1 URA3* (A117V)	19

independently of a GEF. This is mostly explained by reduced GDP affinity or higher dissociation rate constants for GDP release from the G-protein in the absence of GEF. For example, the rate constants for GDP dissociation from both eIF5B and SelB (bacterial EFSec) are higher than other translation factors (5, 6), and eEFSec has lower affinity for GDP (7, 8). This, coupled with the higher level of GTP over GDP in the cell, allows spontaneous regeneration of the active form of the protein (6, 8, 9). Some studies suggest that the ribosome acts as a GEF for prokaryotic RF-3 and EF-G (10). The variety for the GEF requirement and the sequence and structural diversity of GEFs implies that GEF proteins might have gained different functions, which may be specific to the GTPase·GEF complex, cell type or the organism.

One of the G-proteins in the translation family is eukaryotic translation elongation factor (eEF1A). It binds and recruits aminoacyl-tRNAs to the A-site of the ribosome. eEF1A is part of the eEF1 complex, including the eEF1B subunits. eEF1B is composed of the α and γ subunits in fungi, and a third β subunit is present in metazoans. The eEF1Bα subunit performs the catalytic GEF function for eEF1A. The γ subunit is probably a regulatory subunit, since the eEF1Bαγ complex has a proposed role in the oxidative stress response pathway (11). The crystal structure of *Saccharomyces cerevisiae* eEF1A with the catalytic C terminus of eEF1Bα shows that one face of eEF1Bα interacts with domain I, whereas the other interacts with domain II (12). Domain I contains the nucleotide and Mg^{2+} binding site, whereas domain II is the proposed aminoacyl-tRNA binding site of eEF1A. In addition to its established role as a GEF for eEF1A and accelerating the rate of GDP dissociation by 700-fold (13), eEF1Bα also affects translational fidelity (14). Based on the crystal structures of bacterial and eukaryotic EF-Tu/eEF1As, mammalian eEF1A has evolved from bacterial EF-Tu by the insertion of about 70 amino acids into the loop regions between the domains (9). *S. cerevisiae* eEF1A has 81% identity and 89% similarity to human eEF1A (15, 16). These results suggest that although the structure and the function of eEF1A are well conserved, the GEF for eEF1A has gained more complexity and perhaps more functions throughout evolution.

In *S. cerevisiae*, the *TEF5* gene encoding eEF1Bα is essential *in vivo* (17). Interestingly, the requirement for the *TEF5* gene can be suppressed by the presence of excess substrate, eEF1A. Such an eEF1Bα-deficient strain, however, shows defects in growth and translation (18). Two independent, unbiased genetic screens performed to isolate suppressors of the eEF1Bα requirement *in vivo* yielded only eEF1A mutations. The mutant forms of eEF1A that function as suppressors of the eEF1Bα deficiency allow growth similar to a wild type eEF1A strain. In order to analyze the effect of suppressor mutations independent of any other eEF1 components, strains lacking eEF1Bα and both chromosomal eEF1A genes and thus expressing only the mutant form of eEF1A were prepared. Surprisingly, these strains show no growth defects and little to no reduction in total translation (19). Interestingly, all mutations map to the nucleotide-binding domain of eEF1A. Each mutation is in very close proximity to at least one of the conserved sequence elements of the G-protein, which suggests that nucleotide affinity to eEF1A might be affected, creating an open conformation to allow accelerated GDP release without eEF1Bα.

In order to determine the mechanism of the bypass suppression of an essential GEF, we analyzed the effect of mutant forms of eEF1A on nucleotide binding by fluorescence resonance energy transfer (FRET) from hydrophobic residues of eEF1A to fluoresecently 2′-(or 3′)-*O*-*N*-methylanthraniloyl (mant)-labeled nucleotides. The equilibrium dissociation constants (K_d) for mant-GDP binding to eEF1A mutant forms increased up to 37-fold compared with that of wild type eEF1A, indicating reduced GDP affinity. Using stopped-flow kinetics, the mutant forms of eEF1A displayed increased GDP dissociation rates up to 22-fold compared with the wild type protein. However, the K_d values for mant-GMPPNP, a nonhydrolyzable homolog of GTP, were essentially unchanged, indicating that the selective pressure reduces GDP but not GTP binding. Although the mutations do not cause a fundamental change in the native state of the protein as observed by CD spectroscopy, the mutant forms showed dramatically increased stability. Enhanced stability was also observed when eEF1A was bound to guanine nucleotides. Thus, this study demonstrates that the GEF eEF1Bα as well as the distribution of the nucleotide-bound state of eEF1A within the cell probably contribute to stabilizing the protein. The consequences of these eEF1A mutations on the specificity of effects on GDP *versus* GTP binding raises the questions of evolutionary development of GEF function and independence as well as G-protein complexity.

EXPERIMENTAL PROCEDURES

Yeast Techniques and Mutant Preparation—S. cerevisiae strains used in this study are listed in Table 1. *Escherichia coli* DH5α was used for plasmid preparation. Standard yeast genetic methods were employed (20). Yeast cells were grown in YEPD (1% Bacto yeast extract, 2% peptone, 2% dextrose) as the carbon source (21). The R164K, T22S, A112T, and A117V eEF1A mutants were prepared in pTKB754 (*TEF1 URA3*) by PCR mutagenesis using the QuikChange method (Stratagene). The resulting plasmids were transformed into MC213 (*TEF2 TRP1*), loss of wild-type eEF1A plasmid was monitored by growth on 5-fluoroanthranilic acid (22), and the recovered strains

TKY961, TKY963, TKY964, and TKY965, respectively, were used for the purification of the mutant proteins.

Protein Purification—eEF1A was purified as described (13, 23) from strains TKY368, TKY961, TKY963, TKY964, and TKY965 (Table 1) with the following modifications. The eluted and dialyzed material from the protein solution was applied to CM-52 cation exchanger, pre-equilibrated with buffer 1 (20 mM Tris, pH 7.5, 0.1 mM EDTA, pH 8.0, 25% glycerol, 1 mM dithiothreitol, 0.2 mM phenylmethylsulfonyl fluoride, and 1 μg/ml aprotonin). The CM-52 column was washed with buffer 1 with 50 mM KCl and eluted using a 50–300 mM KCl salt gradient of buffer 1. eEF1A-containing fractions were dialyzed overnight against 10 volumes of buffer 1 with 100 mM KCl and stored in aliquots at −80 °C. Protein fractions used for assays were >95% pure, as determined by SDS-PAGE.

Mant-labeled Guanine Nucleotide Binding Assay—Mant-GMPPNP and mant-GDP were both purchased from Molecular Probes and purified with a 1-ml Hi-Trap DEAE-Sepharose Fast Flow column (Amersham Biosciences) using an AKTA fast protein liquid chromatography system (Amersham Biosciences). Nucleotide-containing fractions were combined, lyophilized using a speed vacuum, resuspended in 100 μl of distilled H_2O, and stored at −20 °C (13).

The binding affinity for mant-GDP or mant-GMMPNP to wild type or the mutant forms of eEF1A was measured by a fluorimetric titration assay using a FluoroMax-3 spectrofluorimeter (Horiba Jobin Yvon Inc.). All assays were performed at 25 °C. Wild type or mutant forms of eEF1A (1 μM) in 2.5 ml of binding buffer (10% glycerol, 50 mM Tris-HCl, pH 8.0, 50 mM KCl, and 5 mM $MgCl_2$) were placed in a 10 × 10 × 40-mm quartz cuvette with a magnetic stirring bar. Increasing concentrations of mant-nucleotide were added with continuous stirring for 3 min. Fluorescence changes of the mant-nucleotides (F_{obs}) were monitored upon indirect excitation via FRET. FRET excited tryptophans or tyrosines of eEF1A at a wavelength of 280 nm, and the emission wavelength of 440 nm was for the mant moiety of the nucleotides. The slit widths were 1.05 nm for both wavelengths. The protein and nucleotide complex-dependent fluorescence values (F_{em}) were obtained by correcting for titration volume and inner filter effect using the equation $F_{em} = F_{obs} \times (V_f/V_o) \times 10^{(0.5(Ab_{ex(280)} + Ab_{em(440)}))}$, plotted against mant-GMPPNP or mant-GDP concentrations, and fit to the equations $F_{em} = C + f_{Eb}E_b + f_M M_t$ and $E_b = (K_d + M_t + E_t - (((K_d + M_t + E_t)^2 - 4M_tE_t)))^{0.5}/2$, where V_f is the final volume, V_o is the initial volume, $Ab_{ex(280)}$ is the excitation absorbance of mant-nucleotide, and $Ab_{em(440)}$ is the emission absorbance of mant-nucleotide, C is background fluorescence, f_M is the fluorescence coefficient of free mant-nucleotide, f_{Eb} is the fluorescence coefficient of mant-nucleotide bound to eEF1A, E_t is the total eEF1A protein concentration, M_t is the total concentration of mant-nucleotide, the concentration of eEF1A bound to mant-nucleotide is E_b, and K_d is the mant-GMPPNP or mant-GDP dissociation constant.

Fluorescence Stopped-flow Kinetic Experiments—Stopped-flow experiments using mant-GDP (Molecular Probes) were done in a SF-2001 (KinTek Corp.) stopped-flow spectrophotometer equipped with a photomultiplier detection system as described in Ref. 13.

CD Measurements—CD measurements were made using a circular dichroism spectrometer (model 400; Aviv Biomedical Inc.). The protein concentrations of the purified fractions were determined from the measurement of their different spectra in 6 M guanidine HCl between pH 12.5 and pH 6.0. The molar concentration (MC) of protein in the cuvette was calculated using the formula $MC = A/(2.357Y + 830W)$, where A is the absorbance at 294 nm, Y is the number of tyrosines, and W is the number of tryptophans. The stock solutions were diluted to 0.2–0.4 mg/ml in purification buffer 1 (20 mM Tris, pH 7.5, 0.1 mM EDTA, pH 8.0, 25% glycerol, 1 mM dithiothreitol, 0.2 mM phenylmethylsulfonyl fluoride, and 1 μg/ml aprotonin) to a total volume of 300 μl in cells with a 0.1-cm path wavelength. The wavelength was set to 200–260 nm with 0.5-nm intervals. The wavelength measurements were carried out at 25 °C. After the temperature scan at 222 nm to obtain the melting curve, the wavelength scan was measured at 70 °C and 25 °C again after the samples were cooled down to test the refolding properties of the proteins. The CD spectra were analyzed using neural network analysis programs to determine α-helical, antiparallel, and parallel β- structure, turns, and the remainder content of the proteins (24, 25). The Aviv Macro Editor program was used to collect the wavelength spectra as a function of temperature. The cells were equilibrated for 2 min at 5 °C integrals, and the spectra were accumulated three times at a given temperature. The convex constraint algorithm was used to deconvolute the spectra to obtain the minimum number of basis spectra needed to fit the data (26, 27). All CD data were reported in degrees $cm^2\ dmol^{-1}$ ($[\theta]$).

RESULTS

Interactions of Guanine Nucleotides with eEF1A Are Well Represented by the Change in Mant-nucleotide Fluorescence—In order to determine the base-line guanine nucleotide binding characteristics of eEF1A, FRET from tryptophans and tyrosines of eEF1A to the mant fluorophore of GDP or GMPPNP was determined. Enhanced mant-nucleotide fluorescence with eEF1A (Figs. 1*B* and 2*B*) compared with mant-nucleotides alone (Figs. 1*A* and 2*A*) is the indication of FRET between eEF1A and the mant-nucleotides. In order to determine guanine nucleotide binding affinity of eEF1A, K_d values of eEF1A for mant-GDP and mant-GMPPNP were determined by a fluorimetric titration assay. The K_d for mant-GDP binding to eEF1A was determined as 0.095 μM (Fig. 1*B*). This value is in agreement with a K_d of 1 μM for unlabeled GDP and eEF1A (28) and our previously published K_d of 0.18 μM for mant-GDP binding to eEF1A determined by stopped-flow kinetics (13). To determine GTP binding affinity of eEF1A, the mant-labeled nonhydrolyzable analog of GTP, mant-GMPPNP, was used. The previously published K_d of the eEF1A·GTP complex is 0.7 μM (28). The K_d for mant-GMPPNP binding to eEF1A was measured as 0.52 μM (Fig. 2*B*), indicating that mant-GMPPNP binding to eEF1A is a good representation of unmodified GTP binding to eEF1A.

Mutations of eEF1A That Suppress the Requirement for eEF1Bα Reduce GDP Affinity up to 37-fold—All of the mutations that allow eEF1A to function without its guanine nucleotide exchange factor eEF1Bα cluster in the GTP-binding domain (19). In order to determine if these mutations affect

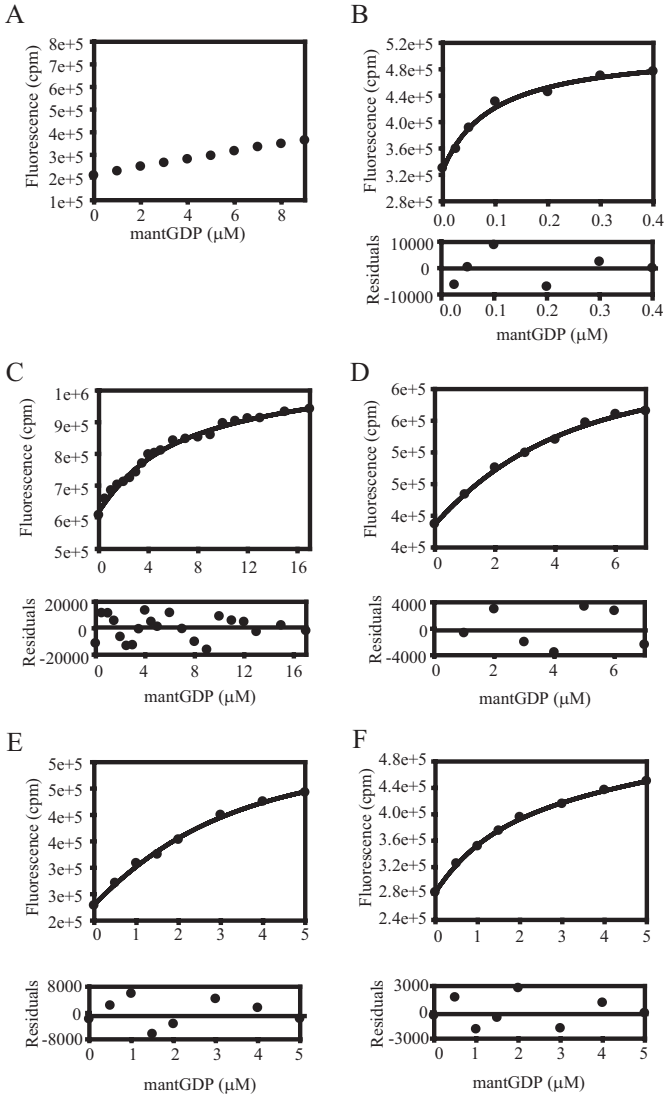

FIGURE 1. **GEF-independent mutants of eEF1A reduce GDP binding.** Equilibrium dissociation constants (K_d) for the mutant forms of eEF1A and mant-GDP were measured. Aliquots of mant-GDP were added to binding buffer without (*A*) or with 1 μM wild type (*B*) or the mutant forms (*C–E*) of eEF1A. The fluorescence was measured by FRET via excitation at 280 nm and emission of 440 nm for mant moiety. Fluorescence intensity (cpm) *versus* the concentration of mant-GDP (μM) was plotted, and data (●) were fit to a hyperbolic curve to obtain the K_d value. The K_d values are measured as 3.54 (T22S) (*C*), 2.66 (R164K) (*D*), 1.80 (A112T) (*E*), and 1.18 μM (A117V) (*F*). Residuals for the fits are shown in the *lower panels* to detect the experimental error for the fitted data sets.

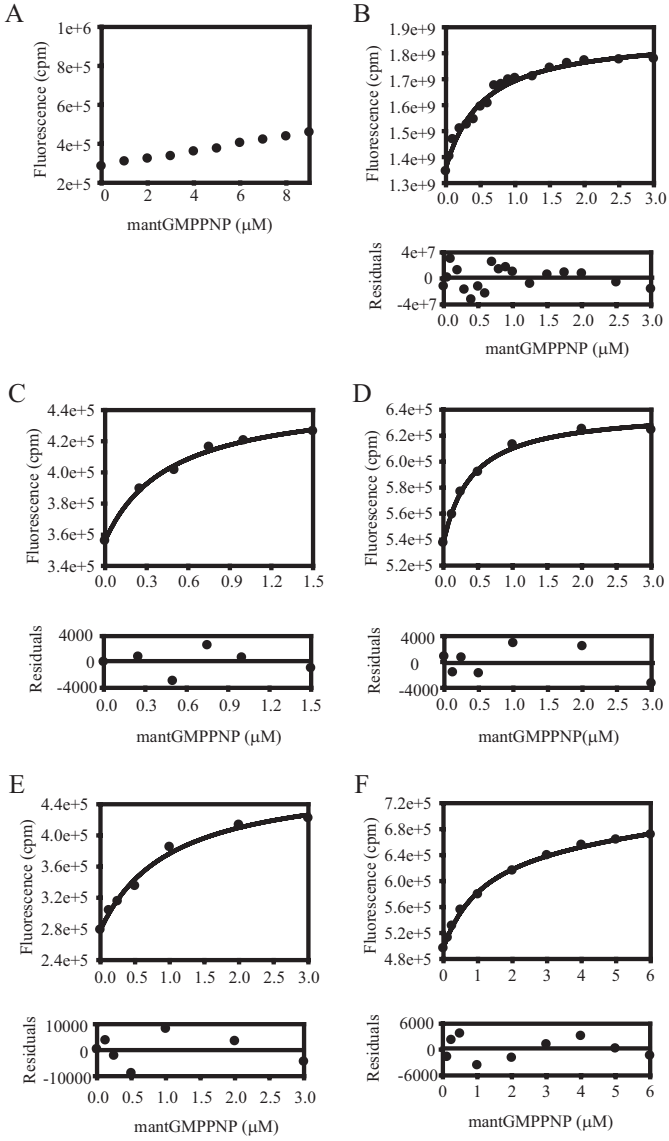

FIGURE 2. **GEF-independent mutants of eEF1A do not affect GMPPNP binding.** The K_d values for the wild type and mutant forms of eEF1A and mant-GMPPNP were measured. Aliquots of mant-GMPPNP were added to binding buffer without (*A*) or with 1 μM of wild type (*B*) or mutant forms (*C–E*) of eEF1A. The fluorescence was measured and plotted as in Fig. 1. The K_d values are measured as 0.47 (T22S) (*C*), 0.41 (R164K) (*D*), 1.01 (A112T) (*E*), and 1.09 μM (A117V) (*F*). Residuals for the fits are shown in the *lower panels* to detect the experimental error for the fitted data sets.

nucleotide affinity in the absence of the exchange factor, we analyzed the GDP binding to the mutant forms of eEF1A by the mant-GDP fluorescence assay. Upon binding of the nucleotide to the eEF1A mutants, an increase in fluorescence was observed, and the data were fitted to determine K_d values for each mutant. The values obtained were 3.54 (T22S), 2.66 (R164K), 1.80 (A112T), and 1.18 μM (A117V) (Fig. 1, *C–F*, and Table 2), which represent a 12–37-fold increase in K_d as compared with wild type eEF1A (0.095 μM; Fig. 1*B*). Thus, one reason for the suppression of the requirement for the guanine nucleotide exchange factor, eEF1Bα, is the reduced affinity of the mutant forms to GDP compared with the wild type eEF1A.

TABLE 2

K_d values for mGDP and GTP, k_{off} for mGDP

	K_d for mGDP	K_d for mGMPPNP	k_{off} for mGDP
	μM	μM	s^{-1}
Wild type	0.095 ± 0.01	0.52 ± 0.02	0.17
T22S	3.54 ± 0.54	0.47 ± 0.19	1.88
R164K	2.66 ± 0	0.41 ± 0.40	2.54
A112T	1.80 ± 0.09	1.01 ± 0.31	1.96
A117V	1.18 ± 0.29	1.09 ± 0.09	3.89

GEF-independent Mutations of eEF1A Do Not Affect GTP Binding— eEF1Bα catalyzes the release of GDP to allow the inactive (GDP-bound) form of eEF1A to recycle back to its active (GTP-bound) form. In order to determine whether these eEF1A mutations reduce binding of both GDP and GTP or specifically GDP affinity, the K_d of the eEF1A mutant proteins

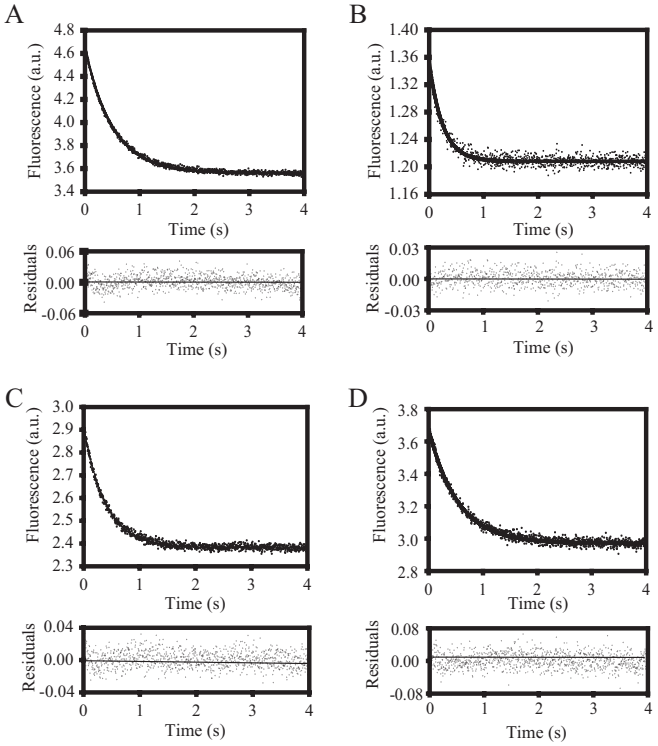

FIGURE 3. **Mutant forms of eEF1A demonstrate faster GDP dissociation.** GDP dissociation rate constants (*k*) for the wild type and the mutant forms of eEF1A were measured. Mutant forms of eEF1A (*A–D*) prebound to mant-GDP were rapidly mixed with excess GDP. The rate of mant-nucleotide release was monitored as a decrease in fluorescent intensity over time and fitted by a single-exponential decay equation to obtain k_{off} values. The k_{off} values are measured as 3.89 (A117V) (*A*), 2.54 (R164K) (*B*), 1.96 (A112T) (*C*), and 1.88 s^{-1} (T22S) (*D*). Residuals for the fits are shown in the *lower panels* to detect the experimental error for the fitted data sets.

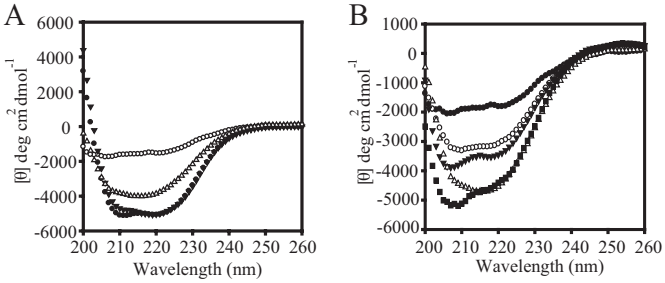

FIGURE 4. **Mutant forms of eEF1A show enhanced thermostability compared with the wild type protein.** The wavelength spectrums of the 0.2–0.4 mg/ml purified proteins are carried out at the indicated temperatures. *A*, circular dichroism spectra of wild type eEF1A (● and ○) and A112T (▲ and △) forms of eEF1A. The *closed symbols* represent the wavelength spectrum at the native state (25 °C), whereas *open symbols* represent the spectrum at 70 °C. *B*, circular dichroism spectra of the mutant forms of eEF1A, R146K (○), T22S (▲), A112T (△), and A117V (■), in comparison with wild type (●) at 70 °C.

for mant-GMPPNP were obtained. The change in fluorescence values was plotted against the increasing concentration of mant-GMPPNP and fitted to the equations to give K_d values of 1.01 (A112T), 1.09 (A117V), 0.47 (T22S), and 0.41 μM (R164K) (Fig. 2, *C–F*, and Table 2). The fact that the K_d values of the mutant forms are very similar to the K_d value of wild type eEF1A (0.52 μM; Fig. 2*B*) indicates that genetic selection during the isolation of the suppressors for the requirement of eEF1Bα targets GDP but not GTP affinity.

GEF-independent Mutants of eEF1A Dissociate GDP at a Higher Rate—To determine if the mutations cause rapid spontaneous GDP dissociation from eEF1A in the absence of its GEF, we measured the dissociation rate constant of the mant-GDP·eEF1A complex using stopped-flow kinetics. Mutant forms of eEF1A were prebound to mant-GDP and then rapidly mixed with an excess of nonfluorescent GDP. The rate of mant-nucleotide release was obtained by monitoring the decrease in fluorescence over time. The fluorescent intensity decayed exponentially on the order of seconds. The time course of mant-GDP displacement from the binary complex of each mutant by excess GDP was fitted by a single-exponential term, yielding dissociation rate constants (k_{off}) of 3.89 (A117V), 2.54 (R164K), 1.96 (A112T), and 1.88 s^{-1} (T22S) (Fig. 3, *A–D*, and Table 2). The average dissociation rate constant of wild type eEF1A is 0.17 s^{-1} (13). These data show that the nucleotide dissociation rate constants were stimulated 11–22-fold in the GEF-independent forms of eEF1A. These results support the contributions of higher GDP release rates in addition to reduced nucleotide affinity in the GEF independence phenotype of a G-protein.

GEF-independent Forms of eEF1A Increase the Thermostability of the Protein—In order to determine if these mutations affect the secondary structure of eEF1A, CD spectroscopy was performed with wild type and mutant forms of eEF1A. eEF1A is α-helical in the GTP binding domain (domain I), whereas domains II and III are composed of antiparallel β-sheets. CD values at 25 °C are plotted against the wavelength to observe the formation of bands for α-helices and β-sheets. There was no difference between the wild type (Fig. 4*A*, ●) and the eEF1A mutant forms, such as A112T (Fig. 4*A*, ▲), which suggest that they all have similar secondary structure.

In addition to providing information on the secondary structural composition of the proteins, CD spectra also allow analysis of unfolding and folding properties of a protein as a function of temperature (29, 30). In order to investigate the thermodynamics of protein folding, the ellipticity was monitored at a single wavelength (222 nm). The resulting melting curves of wild type and the mutant proteins indicated that the mutations caused a different unfolding pattern compared with wild type eEF1A. Intriguingly, the wild type eEF1A completely unfolds at 70 °C (○), whereas the A112T form of eEF1A retained secondary structure (Fig. 4*A*, △). Other mutant forms of eEF1A, R146K (○), T22S (▲), A112T (△), and A117V (■), also increase protein thermostability in comparison with wild type (●) at 70 °C (Fig. 4*B*).

By using neural networks, CD spectra were further analyzed to estimate α-helical, antiparallel, and parallel β- structure, turns, and the remainder content of the proteins. In each mutant, the estimates of the fraction of each secondary structure in native state were similar to the wild type. However, in denatured states, although the α-helical content of wild type protein was reduced to 14% and total β content increased to 35%, the total helix of the mutant forms were up to 20%, and the total β content remained between 25 and 29% (Table 3).

To obtain true thermodynamic properties by CD or other spectroscopic techniques, unfolding and the folding of a protein should be reversible. After melting, the eEF1A samples

were cooled down to 25 °C, and CD spectra at 25 °C showed that unfolding of eEF1A is irreversible. Thus, complete CD spectra as a function of temperature were collected to determine the relative stability by comparing the unfolding intermediates of the wild type and the mutant forms (27). To determine unfolding transitions, a macro writing program was run from 25 to 75 °C with 5 °C intervals, and the wavelength scan was obtained at a range of 200–260 nm at each temperature. To analyze the change in the spectrum of the proteins as a function of temperature, the CD spectra at different temperatures were deconvoluted by the convex constraint algorithm. The minimum number of basis spectra to fit the data were determined to be three, which corresponds to the number of transition states of unfolding. The graphs obtained after deconvolution of the spectra showed that the first intermediates of the unfolding (■) are similar between the wild type (Fig. 5*A*) and the mutant proteins (Fig. 5, *B–E*). The second intermediates (△), however, show that the wild type protein has a distinct peak below 210 nm (*arrow*), corresponding to more β-sheet characteristics not seen in the mutants. Although the third state (●) of wild type eEF1A shows a completely unstructured protein (Fig. 5*A*), some of the secondary structure was protected at the third state of the mutant proteins in correlation with the percentage compositions of the secondary structures (Fig. 5, *B* (A112T), *C* (R164K), *D* (A117V), and *E* (T22S)). The fractions of each curve indicate that at around 40–50 °C, both mutant and wild type proteins leave the first state of the transition and move to the second state. Between 50 and 55 °C, the third states of the proteins emerge.

TABLE 3

Analyses of the structure of wild type and the mutant forms of eEF1A from the CD data in native and denatured states of the proteins

Values represent the percentage of each secondary structure. N, native; D, denatured.

eEF1A forms	Helix total		β total		Turns		Other	
	D	N	D	N	D	N	D	N
Wild type	25	14	23	35	18	19	39	45
A112T	24	21	23	26	18	19	40	43
A117V	24	20	23	25	18	20	40	43
T22S	24	18	23	28	18	20	40	46
R164K	24	17	23	29	18	20	40	46

The unfolding of a protein usually starts with α-helical segments turning into β-sheets. The higher β-sheet content of the second intermediate of wild type eEF1A indicates that the wild type protein starts to denature earlier than most of the mutant proteins. Interestingly, the deeper curve and higher negative values of ellipticity of the wild type protein moving to the third state of the transition as the unfolded state differs from the mutant proteins. The mutant proteins have a third intermediate, which corresponds to a state between the second and third states of wild type eEF1A. A112T and R164K forms of the proteins also delay the transitions by 2–5 °C as compared with the wild type protein, corresponding to the higher values of midpoint of the unfolding transitions (T_M).

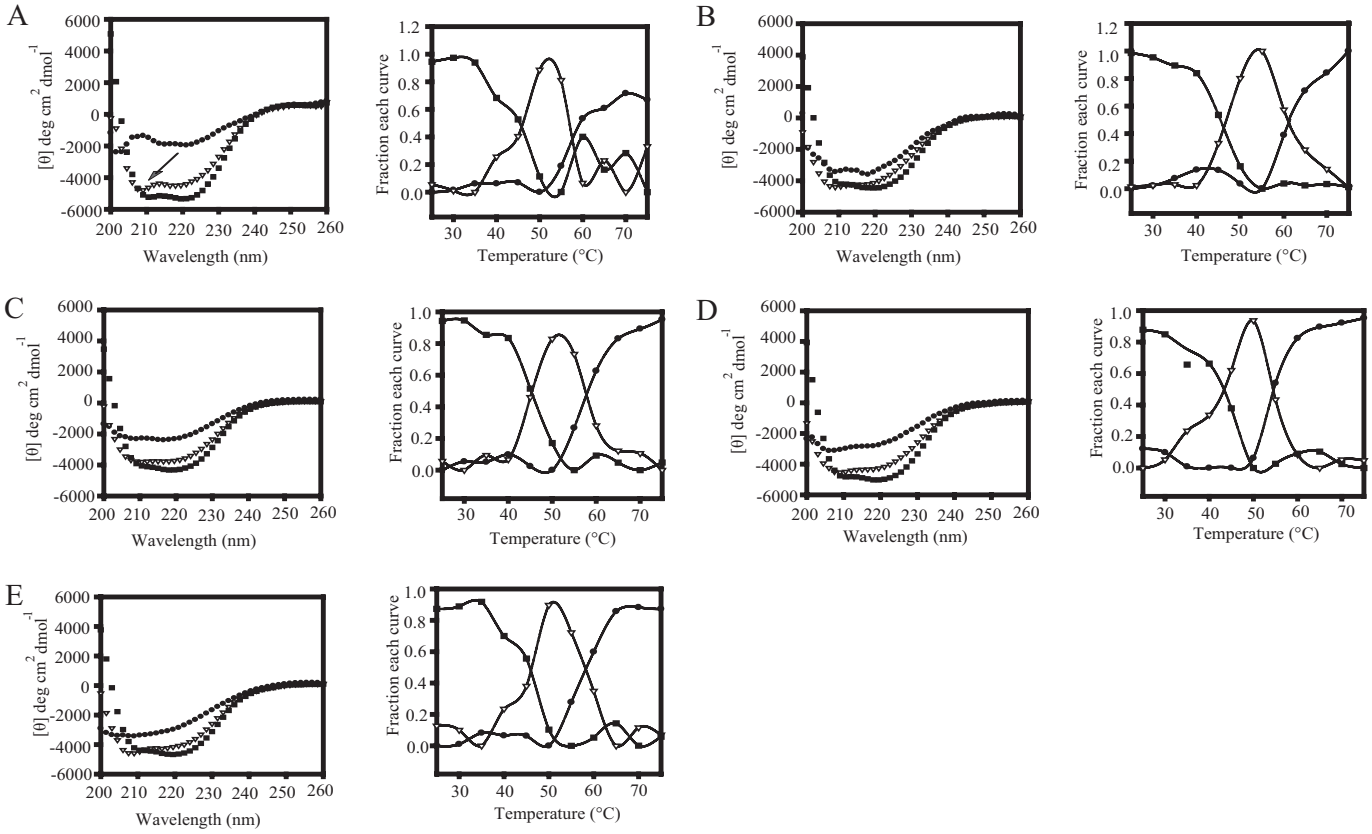

FIGURE 5. **GEF-independent mutants increase eEF1A stability.** Unfolding intermediates of the wild type (*A*), A112T (*B*), R164K (*C*), A117V (*D*), and T22S (*E*) forms of eEF1A measured by circular dichroism spectra and collected as a function of temperature (*left*). The spectra were deconvoluted into three basis curves using the convex constraint algorithm. Each curve (■, △, and ●) represents a different state of unfolding. The *right panel* shows the fraction of each basis curve contributing to each spectrum at each temperature.

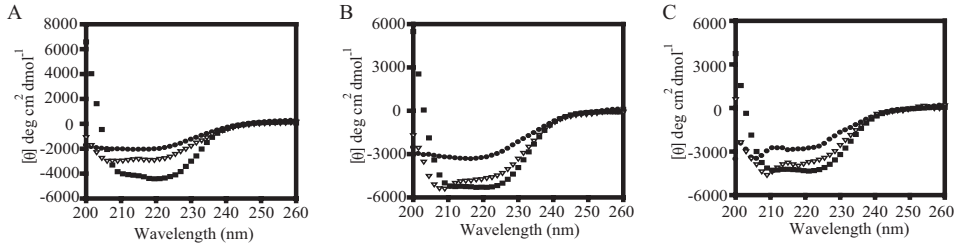

FIGURE 6. **Guanine nucleotides increase eEF1A stability.** Circular dichroism spectra of apo-eEF1A (*A*), eEF1A with GDP (*B*), and eEF1A with GMPPNP (*C*) were measured. The spectra were deconvoluted into three basis curves using the convex constraint algorithm. Each curve (■, △, and ●) represents a different state of unfolding.

Nucleotides Stabilize eEF1A—EF-Tu, the bacterial homolog of eEF1A, is reported to be more stable in the presence of the nucleotides (31). Since the mutations reduce nucleotide affinity but increase the stability of eEF1A, we measured CD spectra of eEF1A in the presence of GDP and GMPPNP to determine the effect of nucleotides on eEF1A stability. The measured K_d value for GTP·eEF1A is 1 μM and that of GMPPNP·eEF1A is 0.7 μM in the presence of 1 μM eEF1A. Therefore, a 5-fold excess of nucleotides were incubated with purified eEF1A to ensure binding. Spectra collected as a function of temperature showed that the first intermediates of the unfolding (■) of apo-eEF1A (Fig. 6*A*) or for eEF1A in the presence of GDP (Fig. 6*B*) or GMPPNP (Fig. 6*C*) are similar with high negative ellipticity values. However, as the proteins move to the second intermediate (△), the apoprotein loses the peaks at specific wavelengths. Both nucleotide-bound forms show a distinct peak close to 210 nm, indicated by *arrows*. This peak probably indicates the presence of secondary structure, mostly β-sheets. At the third state of transition (●), both the apo and GDP-bound forms of the eEF1A have lost the secondary structure, but the GMPPNP-bound form still shows the negative peaks. The fractions of each curve for eEF1A in the presence of nucleotide are similar to the mutant forms (data not shown). These results indicate that eEF1A is more stable when it is bound to the nucleotides, and the GTP-bound form of the eEF1A is the most stable form of all three.

DISCUSSION

Most G-proteins have accessory proteins, which help to regulate their activity via the classic "molecular switch." However, some G-proteins can perform nucleotide exchange with no requirement for a GEF. In addition, although G-proteins form well conserved families and hydrolyze GTP by similar mechanisms, GEFs form a diverse group of molecules (3). To investigate the underlying causes for the GEF requirement of different G-proteins, we analyzed a GEF-independent G-protein system created based on an unbiased genetic screen. Data reported here indicate that genetic selection targets nucleotide affinity and release rates, which is consistent with studies showing that the binding affinity for the nucleotides and the association/dissociation rates account for naturally occurring GEF independence (5, 6).

The assays performed with fluorescently labeled nucleotides to assay eEF1A·GTP and eEF1A·GDP binding demonstrate that these nucleotides are a good representation of nucleotide binding. The mutant proteins have up to 37-fold lower affinity for GDP compared with the wild type protein with little effect on the GMPPNP affinity. Examination of the structure of the eEF1A·eEF1Bα complex in the presence of nucleotides explains the lower affinity of the mutations. The altered residues most likely change the electrostatic interactions of the phosphate groups and/or the guanine base of GDP to the conserved elements of the G-domain of eEF1A.

The interactions of the amino acid residues and the putative effect of the mutations on the structure of eEF1A were evaluated using the PyMol program (32) and DeepView/Swiss-Pdb viewer (33). According to these analyses, Thr-22 forms a hydrogen bond with the α-phosphate of GDP (Fig. 7*A*). In the T22S mutant, disruption of this interaction is predicted to cause GDP to dissociate easily. The T22S mutant has the largest K_d, correlating with its critical position in the structure of eEF1A. GDP binding is most reduced in this mutant, and the GDP dissociation rate is the lowest.

Arg-164 is as close as 5.7 Å to the NK*X*D element of eEF1A (Fig. 7*B*), suggesting that it may play an important role in increasing the affinity of the guanine base. The K_d for GDP in the R164K mutant is reduced less than T22S, but the k_{off} is increased about 33% compared with T22S.

The Ala-117 and Ala-112 residues are located at the upper and lower tip of the same β-strand, which is between a β-strand that connects to the P-loop and a second β-strand that connects to the NK*X*D element (Fig. 7*B*). This could explain why mutations A112T and A117V have similar K_d values for GDP (Table 2). Ala-117 is located between the Ile-116 and Gly-118 residues that interact with NK*X*D via hydrogen bonds, and Ala-117 itself is only 4.3 Å away from the NK*X*D element. Since the NK*X*D motif stabilizes the guanine base, a disruption of these interactions may cause an open conformation aiding in the release of GDP. This is most pronounced for the A117V mutation, which has the highest k_{off} for GDP. The distance between Ala-117 and Arg-164 is the shortest among all pairs of mutations. The distance between Ala-112 and the P loop is 8.9 Å, but Ile-13, the first residue before the P loop, is only 5 Å away from the Ala-112. Therefore, A112T could also allow the P-loop to move and facilitate GDP release without eEF1Bα insertion (Fig. 7*A*). The consequences of the disruption of these critical interactions point out the crucial role of the P-loop and the NK*X*D element for the exchange mechanism.

The mutant eEF1A·nucleotide binding data indicate that the genetic selection for GEF independence targets GDP affinity and that GTP affinity remains unaltered. This result correlates with the effect of eEF1Bα on the nucleotide affinity of eEF1A. eEF1Bα catalyzes the exchange reaction by increasing the rate of GDP dissociation up to 700-fold (13). However, this effect is only related to GDP and not GTP affinity.[3] These data show that the GEF-independent mutants mimic the wild type

[3] S. B. Ozturk and T. G. Kinzy, unpublished data.

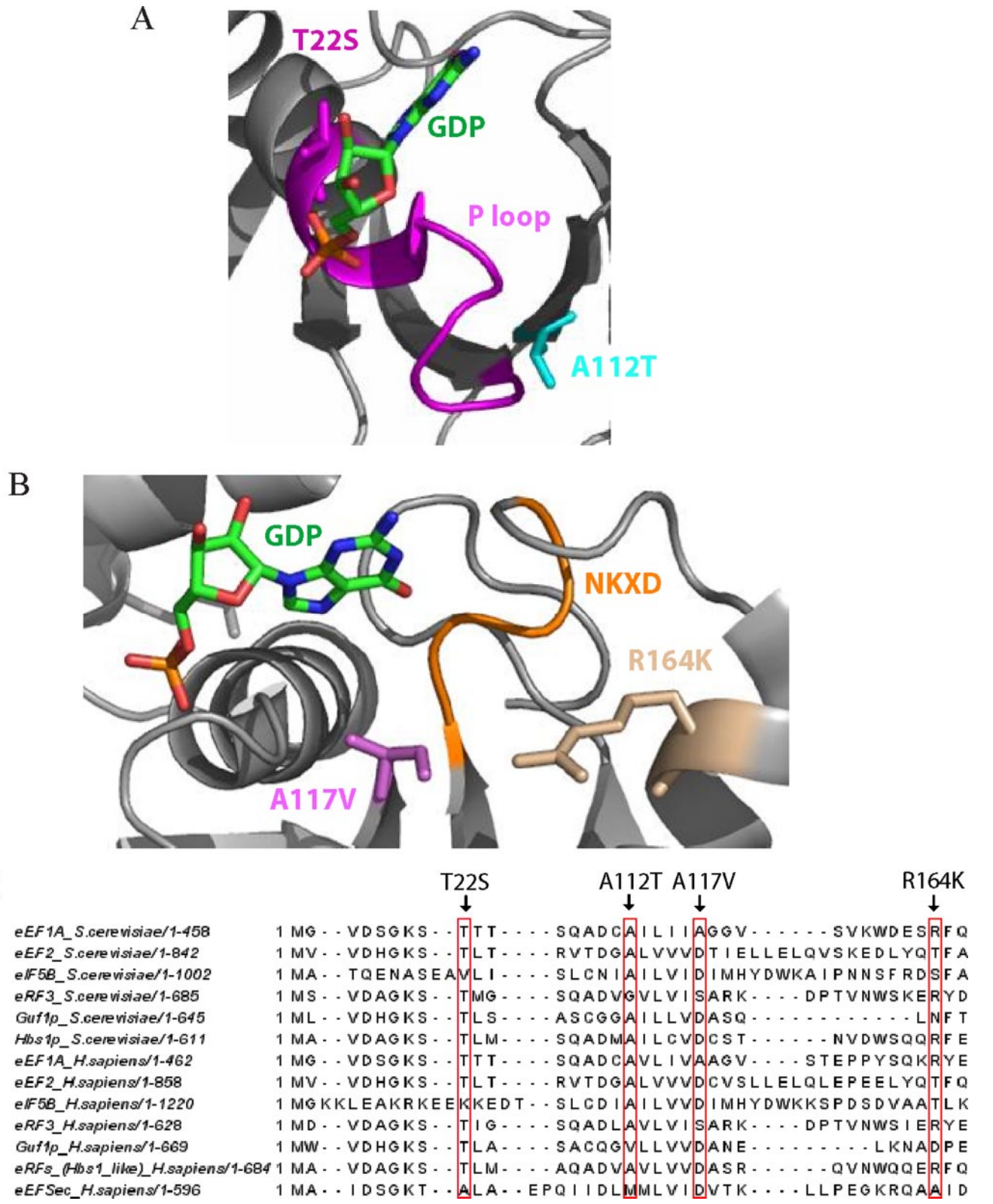

FIGURE 7. **GEF-independent mutants of eEF1A either affect the P-loop or the NK*X*D element.** *A*, Thr-22 (*magenta*) and Ala-112 (*cyan*) residues and their positions respective to the nucleotide (*green*) and the P-loop (*magenta*) are shown. *B*, Arg-164 (*wheat*) and Ala-117 (*purple*) residues and their positions respective to the nucleotide (*green*) and the NK*X*D motif (*yellow*) are shown. The structure was produced with the PyMOL program (32), using the co-crystal structure of the eEF1A·eEF1Bα complex with GDP (Protein Data Bank code 1IJE) (39). *C*, sequence alignment of yeast eEF1A with the G-proteins independent of GEF in yeast (eEF2, eIF5B, eRF3, Guf1p, and Hbs1p) and human (eEF2, eIF5B, eRF3, Guf1p, Hbs1-like eRFs, and eEFSec). The alignment was generated by Jalview (41).

exchange factor complex at least for the interaction with the guanine nucleotides. Although the mutations increase the rate of dissociation up to 22-fold compared with wild type eEF1A, it seems that the combination of both reduced affinity and the higher rates of nucleotide dissociation result in the GEF-independent phenotype. For R164K, A112T, and A117V mutant forms, lower dissociation rates are compensated for by a greater reduction in GDP binding. Although the reduced binding affinity has been suggested to be the reason for the higher dissociation rates, they might be two independent but coordinated events compensating each other to keep the exchange rate above a certain threshold for viability. Interestingly, T22S and A112T forms of eEF1A, which showed the smallest increase in the k_{off} compared with the other two mutants, also have reduced translation efficiency (19). This finding suggests that reduced exchange activity usually correlates with lower translation rates. Overall, the mutations modulate the electrostatic interactions such that eEF1A, on its own, allows the exchange reaction to occur at a sufficient rate for the maintenance of cellular functions. This provides functional information on how cellular systems are dynamically regulated and readily adapt to the limiting conditions.

Most G-proteins are reported to be unstable without bound nucleotides and exchange factors (31, 34, 35). This is probably because most enzymes are more stable and resistant to the proteolysis in the presence of their substrates. The effect of the GEF-independent mutants and guanine nucleotides on the structure of eEF1A was investigated by testing their ability to affect the stability of eEF1A at elevated temperatures. The CD spectra of the mutant and wild type proteins show that GEF-independent forms of eEF1A stabilize a normally unstable protein. Despite many efforts, the crystal structure of the eEF1A without any factor bound has not been solved. This may be a further indication that eEF1Bα stabilizes eEF1A. The eEF1A·GTP complex was more stable than the eEF1A·GDP complex. This finding is consistent with some G-proteins being more thermostable in the GTP-bound conformation than in the GDP-bound conformation, which may be explained by the extra interaction with the γ-phosphate residue of GTP (36, 37). The structures of GTP- and GDP-bound ET-Tu show that a large rearrangement occurs upon GTP hydrolysis (36, 38). In addition, the structure of the eEF1A·eEF1Bα complex resembles GTP-bound EF-Tu (12, 39). A similar closed nature of GTP-bound eEF1A might also account for the greater thermostability of eEF1A in the presence of GTP and the higher stability of the mutant forms of eEF1A in the absence of eEF1Bα. Thus, in addition to modulating nucleotide affinity, GEF-independent forms also increase the stability to perhaps compensate for another role of eEF1Bα. This finding also sheds light on the isolation and designation of the historical bacterial T fraction (the EF-Tu·EF-Ts complex) as two components: one stable component, T_s, and a heat-labile, unstable component, T_u, the bacterial homolog of eEF1A (40).

In addition, thermostability of the mutant forms of eEF1A correlates with the initial conditions of the screens that yielded the suppressors of eEF1Bα deficiency. The eEF1Bα-deficient strain used for the EMS (ethyl methanesulfonate) mutagenesis was thermosensitive and cold-sensitive. In the first screen, the colonies were screened for growth at 37 °C. The resulting mutations all suppressed the temperature sensitive phenotype of the strain overexpressing eEF1A and lacking eEF1Bα but not the cold sensitivity. To avoid this bias, the screen was repeated looking at growth at 24 and 37 °C, and again a significant overlapping group of mutants was obtained compared with the first screen, and all grew better at 37 °C. In fact, suppression was clearly more pronounced at 37 °C (19). Therefore, in this paper, we showed that the *in vitro* characteristics of the proteins are consistent with the *in vivo* phenotype of the strains from the original screen.

In some cases, the affinity of a G-protein for GDP is much higher than the GTP, so the requirement for an exchange factor is obvious. However, the weaker binding of GDP compared with GTP and high dissociation rate constants are an indication for a G-protein without exchange factor dependence, such as for eIF5B and bacterial eEFSec (5, 6). Sequence alignments were analyzed to investigate the potential significance of the differences and the similarities between the GEF-independent G-proteins (eEF2, eIF5B, eRF3, eEFSec, Guf1p, and Hbs1p) and GEF-independent forms of eEF1A. Thr-22 and Ala-112 are both 83% identical between GEF-independent proteins from yeast and 77 and 66% identical between human GEF-independent proteins, respectively. The same residues are 100% conserved in eEF1A/EF-Tu from 11 selected organisms from bacteria to human. The Ala-117 and R164K residues are 85% identical in eEF1A/EF-Tu, and the same residues in human and yeast proteins functioning without a GEF show only a 25–35% identity. Interestingly, other than the Lys substitute for Arg-164 in mitochondrial IF-2, none of the mutations that allow eEF1A to be GEF-independent occur in other GEF-independent proteins (Fig. 7*C*). Thus, there appears to be selective pressure to maintain these residues in the elongation factors. This indicates that the mechanisms that result in altered nucleotide exchange activities between eEF1A and other GEF-independent G-proteins are not same but that eEF1A can also act as a GEF-independent G-protein by remodeling its nucleotide-G-protein interactions at highly conserved sites.

Acknowledgments—We thank the members of the Kinzy laboratory for helpful comments. We thank Yvette Pittman for help with kinetic studies, Dr. Norma Greenfield for assistance in obtaining and analyzing CD spectra, Dr. Smita Patel for use of stopped-flow equipment, and Peter Krueger for the sequence analysis of GEF-independent G-proteins.

REFERENCES

1. Vetter, I. R., and Wittinghofer, A. (2001) *Science* **294,** 1299–1304
2. Dever, T. E., Glynias, M. J., and Merrick, W. C. (1987) *Proc. Natl. Acad. Sci. U. S. A.* **84,** 1814–1818
3. Sprang, S. R., and Coleman, D. E. (1998) *Cell* **95,** 155–158
4. Bos, J. L., Rehmann, H., and Wittinghofer, A. (2007) *Cell* **129,** 865–877
5. Pisareva, V. P., Hellen, C. U., and Pestova, T. V. (2007) *Biochemistry* **46,** 2622–2629
6. Thanbichler, M., Bock, A., and Goody, R. S. (2000) *J. Biol. Chem.* **275,** 20458–20466
7. Tujebajeva, R. M., Copeland, P. R., Xu, X. M., Carlson, B. A., Harney, J. W., Driscoll, D. M., Hatfield, D. L., and Berry, M. J. (2000) *EMBO Rep.* **1,** 158–163

8. Fagegaltier, D., Hubert, N., Yamada, K., Mizutani, T., Carbon, P., and Krol, A. (2000) *EMBO J.* **19,** 4796–4805
9. Merrick, W. C., and Nyborg, J. (2000) in *Translational Control of Gene Expression* (Sonenberg, N., Hershey, J. W. B., and Mathews, M. B., eds) pp. 89–126, Cold Spring Harbor Laboratory, Cold Spring Harbor, NY
10. Zavialov, A. V., Hauryliuk, V. V., and Ehrenberg, M. (2005) *J. Biol.* (*Bronx N. Y.*) **4,** 9
11. Olarewaju, O., Ortiz, P. A., Chowdhury, W., Chatterjee, I., and Kinzy, T. G. (2004) *RNA Biol.* **1,** 12–17
12. Andersen, G. R., Pedersen, L., Valente, L., Chatterjee, I., Kinzy, T. G., Kjeldgaard, M., and Nyborg, J. (2000) *Mol. Cell* **6,** 1261–1266
13. Pittman, Y., Valente, L., Jeppesen, G. R., Andersen, G. R., and Patel, S. (2006) *J. Biol. Chem.* **281,** 19457–19468
14. Carr-Schmid, A., Valente, L., Loik, V. I., Williams, T., Starita, L. M., and Kinzy, T. G. (1999) *Mol. Cell Biol.* **19,** 5257–5266
15. Schirmaier, F., and Phillipson, P. (1984) *EMBO J.* **3,** 3311–3315
16. Anand, M., Valente, L., Carr-Schmid, A., Munshi, R., Olarewaju, O., Ortiz, P., and Kinzy, T. G. (2001) *Symp. Quant. Biol.* **66,** 439–448
17. Hiraga, K., Suzuki, K., Tsuchiya, E., and Miyakawa, T. (1993) *FEBS Lett.* **316,** 165–169
18. Kinzy, T. G., and Woolford, J. L., Jr. (1995) *Genetics* **141,** 481–489
19. Ozturk, S. B., Vishnu, M. R., Olarewaju, O., Starita, L. M., Masison, D. C., and Kinzy, T. G. (2006) *Genetics* **174,** 651–663
20. Burke, D., Dawson, D., and Stearns, T. (2000) *Methods in Yeast Genetics: A Laboratory Course Manual*, Cold Spring Harbor Laboratory, Cold Spring Harbor, NY
21. Ausubel, F. M., Brent, R., Kingston, R. E., Moore, D. D., Seidman, J. G., Smith, J. A., and Struhl, K. (1992) *Current Protocols in Molecular Biology*, pp. 13.0.1–13.14.17, John Wiley & Sons, Inc., New York
22. Toyn, J. H., Gunyuzlu, P. L., White, W. H., Thompson, L. A., and Hollis, G. F. (2000) *Yeast* **16,** 553–560
23. Carvalho, M. G., Carvalho, J. F., and Merrick, W. C. (1984) *Arch. Biochem. Biophys.* **234,** 603–611
24. Bohm, G., Muhr, R., and Jaenicke, R. (1992) *Protein Eng.* **5,** 191–195
25. Unneberg, P., Merelo, J. J., Chacon, P., and Moran, F. (2001) *Proteins* **42,** 460–470
26. Perczel, A., Hollosi, M., Tusnady, G., and Fasman, G. D. (1991) *Protein Eng.* **4,** 669–679
27. Greenfield, N. J. (2006) *Nature Protocols* **1,** 2527–2535
28. Saha, S. K., and Chakraburtty, K. (1986) *J. Biol. Chem.* **261,** 12599–12603
29. Greenfield, N. J. (2006) *Nat. Protoc* **1,** 2876–2890
30. Bhate, M., Wang, X., Baum, J., and Brodsky, B. (2002) *Biochemistry* **41,** 6539–6547
31. Lapadat, M. A., and Spremulli, L. L. (1989) *J. Biol. Chem.* **264,** 5510–5514
32. DeLano, W. L. (2002) *PyMol*, Delano Scientific, San Carlos, CA
33. Guex, N., and Peitsch, M. C. (1997) *Electrophoresis* **18,** 2714–2723
34. Ferguson, K. M., Higashijima, T., Smigel, M. D., and Gilman, A.D. (1986) *J. Biol. Chem.* **259,** 8693–8698
35. Lutz, S., Baltus, D., Jakobs, K. H., and Niroomand, F. (2002) *Naunyn-Schmiedeberg's Arch. Pharmacol.* **365,** 50–55
36. Kjeldgaard, M., Nissen, P., Thirup, S., and Nyborg, J. (1993) *Structure* **1,** 35–50
37. Sanderova, H., Hulkova, M., Malon, P., Kepkova, M., and Jonak, J. (2004) *Protein Sci.* **13,** 89–99
38. Berchtold, H., Reshetnikova, L., Reiser, C. O. A., Schirmer, N. K., Sprinzl, M., and Hilgenfeld, R. (1993) *Nature* **365,** 126–132
39. Andersen, G. R., Valente, L., Pedersen, L., Kinzy, T. G., and Nyborg, J. (2001) *Nat. Struct. Biol.* **8,** 531–534
40. Lucas-Lenard, J., and Lipmann, F. (1966) *Proc. Natl. Acad. Sci. U. S. A.* **55,** 1562–1566
41. Clamp, M., Cuff, J., Searle, S. M., and Barton, G. J. (2004) *Bioinformatics* **20,** 426–427